Laser & Photon. Rev. **4**, No. 1, 160–177 (2010) / **DOI** 10.1002/lpor.200810060

Abstract Grating-based chirped pulse amplifiers are the cornerstone of high-power femtosecond lasers. The amplification of carrier-envelope phase stable pulses in such lasers has only been realized within the last few years. Currently, the state-of-the-art in this endeavor is utilizing the change in grating separation in the stretcher or compressor. The carrier-envelope phase drift can be reduced to the 160 mrad RMS level and the carrier-envelope phase can be swept in a 2π range. The effects of laser pulse energy stability on the f-to-$2f$ measurement of the carrier-envelope phase were found to be significant, with a 1% change in laser energy leading to 160 mrad phase error, showing the need for power-stable amplified laser systems. The phase-stabilized pulses from grating-based chirped amplifiers have been successfully used in attosecond pulse generation with subcycle gating techniques.

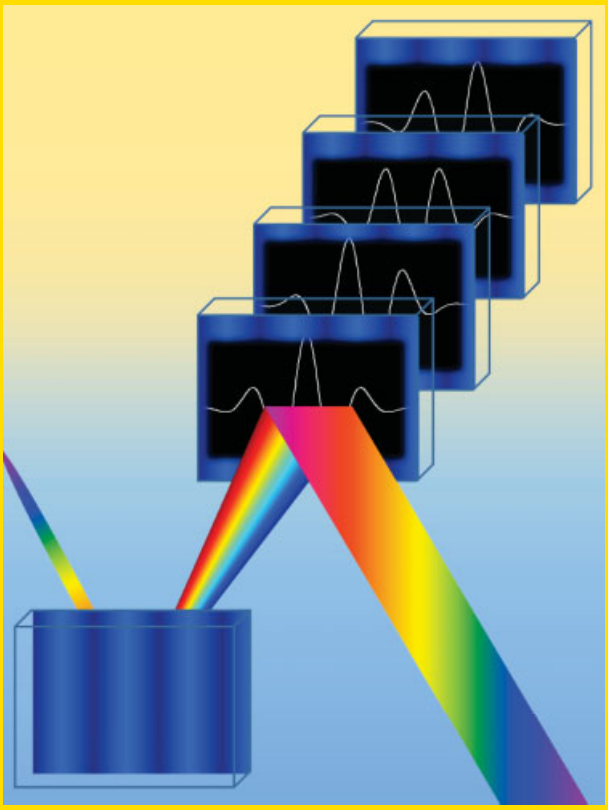

When a laser pulse propagates through a pair of diffraction gratings, its carrier-envelope phase depends strong on the separation of gratings. This effect has been used to stabilize the carrier-envelope phase in chirped pulse laser amplifiers.

Advances in carrier-envelope phase stabilization of grating-based chirped-pulse amplifiers

Eric Moon[1,2], *He Wang*[1], *Steve Gilbertson*[1], *Hiroki Mashiko*[1], *Michael Chini*[1], *and Zenghu Chang*[1,*]

[1] J. R. Macdonald Laboratory, Department of Physics, Kansas State University, 116 Cardwell Hall, Manhattan Kansas 66506, USA
[2] currently at Quantronix in East Setauket, NY, USA

Received: 10 October 2008, Revised: 5 February 2009; 7 April 2009, Accepted: 20 April 2009
Published online: 17 June 2009

Key words: Carrier-envelope phase, few-cycle laser, high-power laser, attosecond pulses, femtosecond, high-harmonic generating, subcycle gating, f-to-$2f$ interferometry.

PACS: 32.80.Qk, 42.30.Rx, 42.65.Ky, 42.65.Re, 42.65.Sf

* Corresponding author: e-mail: chang@phys.ksu.edu

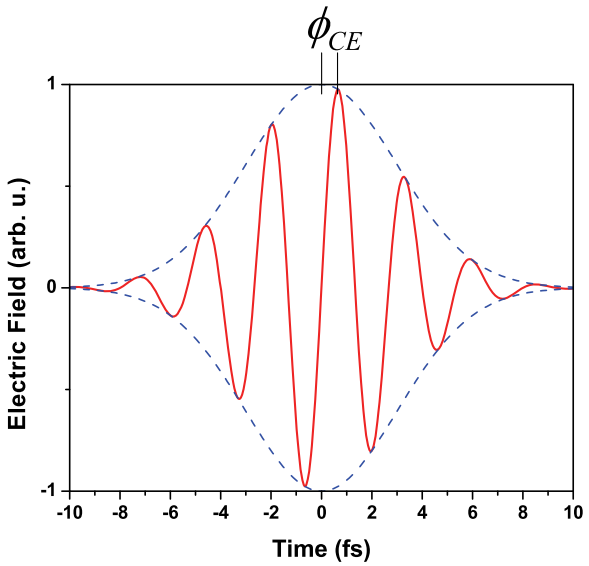

Figure 1 (online color at: www.lpr-journal.org) A few-cycle laser pulse showing the carrier-envelope offset, φ_{CE}.

1. Introduction

In Fig. 1, the electric field of a linearly polarized, few-cycle transform-limited pulse is shown. At a fixed point in space, the field of the laser pulse can be described as $E(t) = A(t)\cos(\omega_0 t + \varphi_{\mathrm{CE}})$, where $A(t)$ is the pulse amplitude, which is peaked at $t = 0$, and ω_0 is the carrier frequency. The carrier-envelope phase, φ_{CE}, denotes the offset between the peak of the pulse envelope and the nearest peak of the carrier-wave electric field.

As the width of $A(t)$ approaches few- or single-cycle duration, the electric-field amplitude changes rapidly within half of the cycle. This fast variation of the electric field within the pulse envelope is the origin of carrier-envelope (CE) phase effects in a variety of high-field processes such as above-threshold ionization and high-order harmonic generation [1, 2]. The CE phase can affect the high-order harmonic-generation process even when the excitation laser is long. The spectrum from the long trajectories was shown to depend strongly on the CE phase when the driving laser was 20 fs [3].

For generating attosecond pulses using polarization gating or double optical gating, the effective electric field inside the gate can be expressed as $E(t) = g(t)\cos(\omega_0 t + \varphi_{\mathrm{CE}})$. Here, $g(t)$ is the gating function with a duration of a fraction of a laser cycle and the center of the gate occurs at $t = 0$. In these cases, the opening time of the gate for single attosecond pulse extraction is of the order of half to one cycle [4–6]. Thus, it is crucial to stabilize and control the CE phase. In Sect. 6 of this paper, the effects of CE phase on polarization gating and double optical gating will be explored in detail.

Other processes are also susceptible to the CE phase. For example, CE phase effects have been predicted in the dissociation of molecules [7] and in electron emission from metal surfaces [8]. CE phase even played a role in terahertz-emission spectroscopy with few-cycle pulses [9]. Advances in CE phase control have allowed researchers access to controlling such processes as injected photocurrents in semiconductors [10] and in sub-single-cycle pulse trains generated with Raman sidebands [11].

A typical laser system for generating few-cycle CE phase-stabilized pulses is shown in Fig. 2. First, the CE phase evolution in the oscillator is stabilized and the pulses with the same CE phase are selected and sent to the amplifier, after they are temporally stretched. After amplification, the pulses are recompressed in time and the CE-phase drift introduced by the amplifier is then corrected. The laser pulses are then spectrally broadened through a nonlinear process. The pulses are then compressed to only a few cycles in duration. Finally, the CE phase of the few-cycle pulses is measured. This scheme is used by almost all groups in the ultrafast field to obtain high-energy, few-cycle, CE-phase stable pulses.

Currently, commercially available Ti:sapphire laser oscillators can produce <10 fs pulses [12]. The durations of amplified laser pulses are typically around 30 fs, due to gain narrowing, which can be shortened to ~ 5 fs in hollow-core fiber/chirped-mirror compressors [13–15] or filamentation setups [16, 17]. Also, adaptive phase modulation in conjunction with spectral broadening in a hollow-core fiber

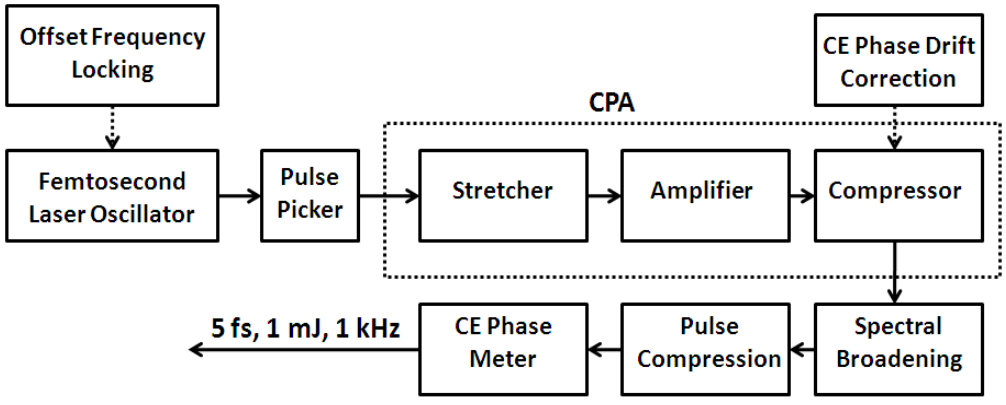

Figure 2 A schematic diagram of a CE-phase stable laser system producing few-cycle pulses.

filled with neon gas has been shown to produce high-power two-cycle pulses [18].

In this paper, the various methods used to stabilize and control the CE phase in femtosecond Ti:sapphire laser oscillators and amplifiers will be reviewed. The main focus of the article will be on the advances made in CE phase control and stabilization of grating-based Ti:sapphire chirped-pulse amplifiers. The usefulness of the CE phase-stabilized pulses from such lasers is shown in attosecond pulse generation with double optical gating.

2. Dispersion and CE phase variation

Dispersion of optical elements in the laser beam path causes the CE phase to shift. The effects of the dispersion introduced by the gratings in the stretcher and compressor on the CE phase will be discussed in Sect. 4. Here, the CE-phase shift in a linear homogenous optical medium is discussed. Mathematically, the CE-phase offset acquired by the pulse in one pass through a linearly dispersive medium can be expressed as:

$$\Delta\varphi_{\mathrm{CE}} = \Delta\varphi_{\mathrm{g}} - \Delta\varphi_{\mathrm{p}} = \omega_0 \left[\frac{L_0}{v_{\mathrm{g}}(\omega_0)} - \frac{L_0}{v_{\mathrm{p}}(\omega_0)}\right] = -2\pi L_0 \left.\frac{\mathrm{d}\,n}{\mathrm{d}\,\lambda}\right|_{\omega_0}, \quad (1)$$

where $\Delta\varphi_{\mathrm{g}}$ and $\Delta\varphi_{\mathrm{p}}$ are phase shifts caused by the group and phase delay, respectively. v_{g} and v_{p} are the group and phase velocity. L_0 is the length of the dispersive medium and n is the index of refraction. Thus, the phase velocity of the carrier wave and the group velocity of the laser pulse are different due to dispersion, which leads to a CE-phase shift. For example, $\sim 15\,\mu$m of fused silica will impart a $\frac{\pi}{2}$ CE-phase shift to a laser pulse. The material dispersion thus has an important ramification for both oscillators and amplifiers. Note also that Eq. (1) does not take into account the nonlinear contribution to the CE-phase shift. The nonlinear contribution will be discussed in an upcoming section as it provides a mechanism for CE-phase stabilization [19]

3. Stabilization of the CE phase change rate in laser oscillators

Inside a femtosecond oscillator cavity, a laser pulse circulates through the gain medium, reflects off the various mirrors, and finally passes through the output coupler. The main dispersive elements in a chirped-mirror-based Kerr-lens mode-locked (KLM) Ti:sapphire laser are the laser crystal, the air in the laser path and the mirrors. For a typical Ti:sapphire oscillator operating at a repetition rate of $\sim$ 80 MHz, the air path is ~ 2 m and the crystal is ~ 2 mm thick. A KLM Ti:sapphire laser can also be operated with prisms for dispersion compensation, which would also contribute to changing the group and phase velocities [20]. Since the phase and group velocities differ, the CE-phase offset will change from one round trip to the next, as shown in Fig. 3. Because of this, it is technically difficult to lock the CE phase of all the oscillator pulses to the same value. Instead, in most cases the change rate of the CE phase is stabilized. The pulses with the same CE phase are then selected by the Pockels cell to seed the amplifier.

3.1. Carrier-envelope offset frequency

The previous discussion described the CE-phase offset only in the time domain. However, the CE-phase offset also has a major effect in the frequency domain. In the temporal domain, a mode-locked laser pulse train is just a steady stream of pulses separated by $T = \frac{1}{f_{\mathrm{rep}}}$, where T is the

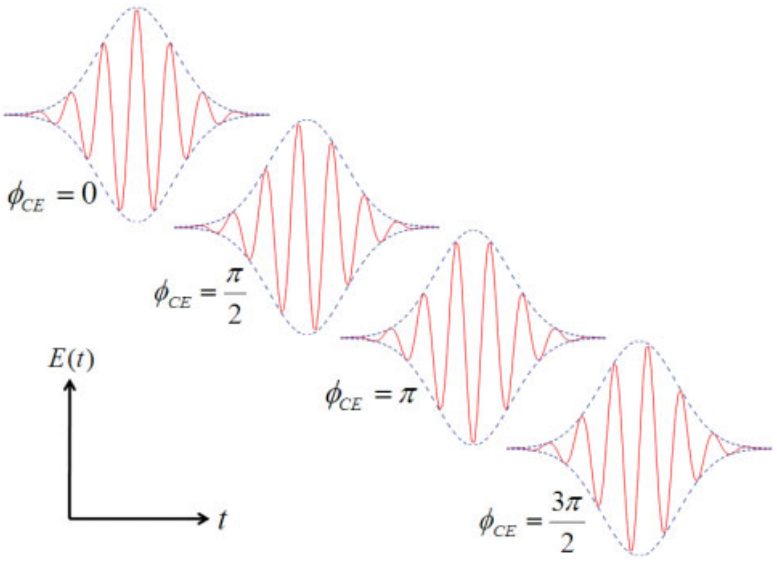

Figure 3 (online color at: www.lpr-journal.org) Four pulses with different values of the CE phase.

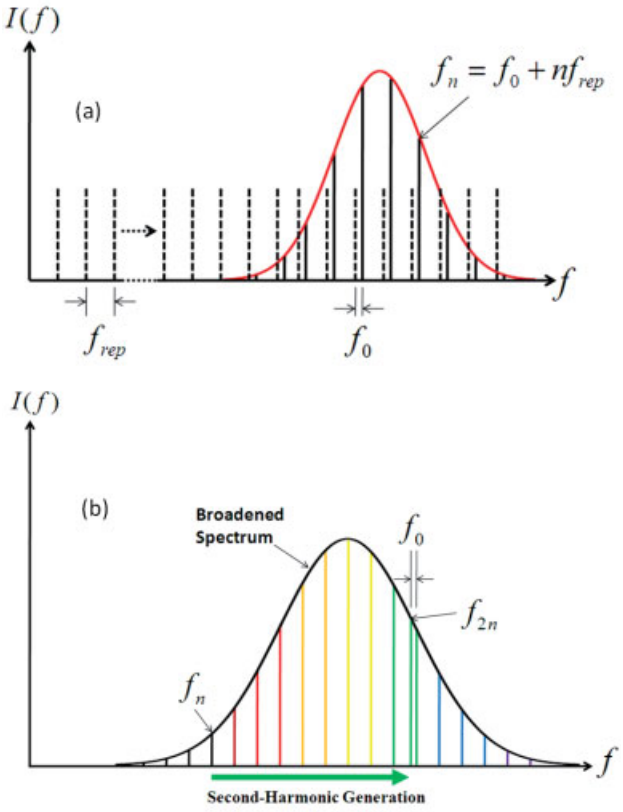

Figure 4 (online color at: www.lpr-journal.org) a) The frequency comb and the offset frequency. The comb lines are shifted by f_0 underneath the laser spectrum. b) f-to-$2f$ self-referencing technique. f_n is frequency doubled. f_0 is the difference between f_n and f_{2n}.

pulse period and $f_{\rm rep}$ is the laser repetition rate. In the frequency domain, the pulse train appears as a set of equally spaced comb lines within the laser spectrum separated by $f_{\rm rep}$. The cavity modes are given by:

$$f_n = f_0 + nf_{\rm rep}\,, \tag{2}$$

where f_0 is an offset frequency resulting from dispersion in the cavity and is directly related to the roundtrip CE-phase shift as will be shown.

If the phase and group velocities of the laser pulse and field in the cavity are equal, then f_0 is equal to zero. The situation is depicted in Fig. 4a, where the dashed lines represent the equally spaced comb lines and the solid lines underneath the laser spectrum represent the dispersion shifted comb lines [21]. Ref. [21] provides a mathematical derivation of how including a CE-phase shift in the description of the pulse train and then performing a Fourier transform to the frequency domain results in an offset frequency. Similarly, a simple argument can give the relationship between the offset frequency and the pulse-to-pulse CE-phase shift.

The phase of the nth cavity mode is given by:

$$\psi_n(t) = 2\pi f_n t = 2\pi f_0 t + 2\pi n f_{\rm rep} t\,. \tag{3}$$

Now, consider the phase of the mode after the pulse completes one cavity round-trip. The phase of the mode is given by:

$$\psi_n\left(t+\frac{1}{f_{\rm rep}}\right) = 2\pi f_n\left(t+\frac{1}{f_{\rm rep}}\right) = 2\pi f_0 t + 2\pi n f_{\rm rep} t + 2\pi\frac{f_0}{f_{\rm rep}}\,. \tag{4}$$

Comparing Eqs. (3) and (4), after one cavity round-trip each mode acquires an extra phase shift, which is the CE-phase shift and is denoted by:

$$\Delta\varphi_{\rm CE} = \frac{2\pi f_0}{f_{\rm rep}}\,. \tag{5}$$

All the laser modes, and thus a pulse after a cavity round-trip, will undergo a phase shift equal to Eq. (5). Note that according to Eq. (5) the CE-phase shift is mode-index independent [22]. Therefore, the presence of dispersion in a laser cavity results in an offset frequency in the frequency domain that has a simple relationship to the CE phase. As will be shown in the next section, this offset frequency, along with optical techniques can be used to stabilize the CE-phase shift.

3.2. Carrier-envelope offset frequency stabilization

Nowadays, the technology of stabilizing the CE phase of mode-locked Ti:sapphire lasers is well established. Methods exist for CE-phase stabilization of octave-spanning oscillators [23]. CE-phase technology has come very far since the first attempt at measuring the CE-phase shift between successive pulses from a Ti:sapphire oscillator using a second-order crosscorrelator [24]. Most of the current methods used to stabilize the CE phase were first addressed in [25], where different nonlinear processes and the respective spectral bandwidth requirements were compared. It was deduced that frequency doubling the low comb orders and heterodyne beating with the comb orders in the high-frequency spectrum would produce f_0. Second-harmonic generation would be the simplest method, requiring only one nonlinear process, but this also required an octave-spanning spectrum, which was unavailable at the time [25]. This was called the f-to-$2f$ self-referencing method.

In fact, shortly after microstructure fibers with zero-dispersion points in the near infrared were introduced, it was shown that an octave-spanning spectrum could be produced through the nonlinear processes induced by focusing a Ti:sapphire laser into the small core [26]. Then, using such a fiber and an f-to-$2f$ self-referencing method, the offset frequency was measured [27] and electronically controlled [20,28]. Of course, other methods exist for obtaining the offset frequency, including difference-frequency generation (0-to-f) and interval bisection [25, 29]. However, the

majority of groups use the f-to-$2f$ method, which will be discussed in this section.

Fig. 4b shows the principle of the f-to-$2f$ self-referencing method. The original laser spectrum is broadened over an octave in frequency. Then, the low-frequency components are frequency doubled and interfered with the high comb orders [30]. Mathematically, the heterodyne beat resulting from the aforementioned process can be represented as:

$$2f_n - f_{2n} = 2(nf_{\mathrm{rep}} + f_0) - (2nf_{\mathrm{rep}} + f_0) = f_0\,. \quad (6)$$

Thus, the difference between the f and $2f$ comb orders is the offset frequency.

The next step in the process of locking the CE phase is to track the offset frequency and lock it to either zero frequency [31] or to an integer fraction of the laser repetition rate using a servo loop [32]. Locking the offset frequency to a fraction of the laser repetition rate is the most common method as the repetition rate is easily accessible. Two fast mechanisms can be used to lock the offset frequency to a fixed value. The first method involves tilting a mirror in the cavity to change the path length, which only works for prism-based lasers [33, 34]. The second, and the more common, method is to modulate the pump power with an acousto-optic modulator (AOM). Modulating the pump power changes the nonlinearity in the crystal, which also changes the refractive index and thus the group and phase velocities [35, 36].

3.3. The effects of f-to-$2f$ interferometers

Several studies have been conducted on the quality of CE-phase stabilization systems. It was found that laser-power stability was a factor when determining the offset frequency using a nonlinear fiber [37]. The authors measured the amplitude-to-phase coupling coefficient of the microstructure fiber and found a value of 3784 rad/nJ, which was quite large and showed the need for good laser-power stability. In other research by the same group, they measured the in- and out-of-loop accumulated phase noise when the oscillator was locked and unlocked. It was found that the out-of-loop phase noise was slightly higher due to mechanical vibrations in the optical mounts used to stabilize the CE phase, which indicated the locking servo was writing extra CE-phase noise onto the output pulses [38].

The noise introduced by path-length fluctuation in the interferometer used to stabilize the CE phase was also investigated [39]. A change in path length, due to air fluctuation or vibration of the mirror mounts, would lead to fluctuations in the detected offset frequency. In turn, even with the CE-phase-locking system working perfectly, the noise from the path-length drift would still cause a CE-phase shift of the pulses leaving the oscillator. In order to investigate the path-length variation, a helium-neon laser beam was copropagated with the Ti:sapphire beam through the interferometer to obtain an interference pattern directly related to the path-length variation. The experimental setup is shown in Fig. 5. The interference signal was used to lock the interferometer path length via a PZT-mounted mirror

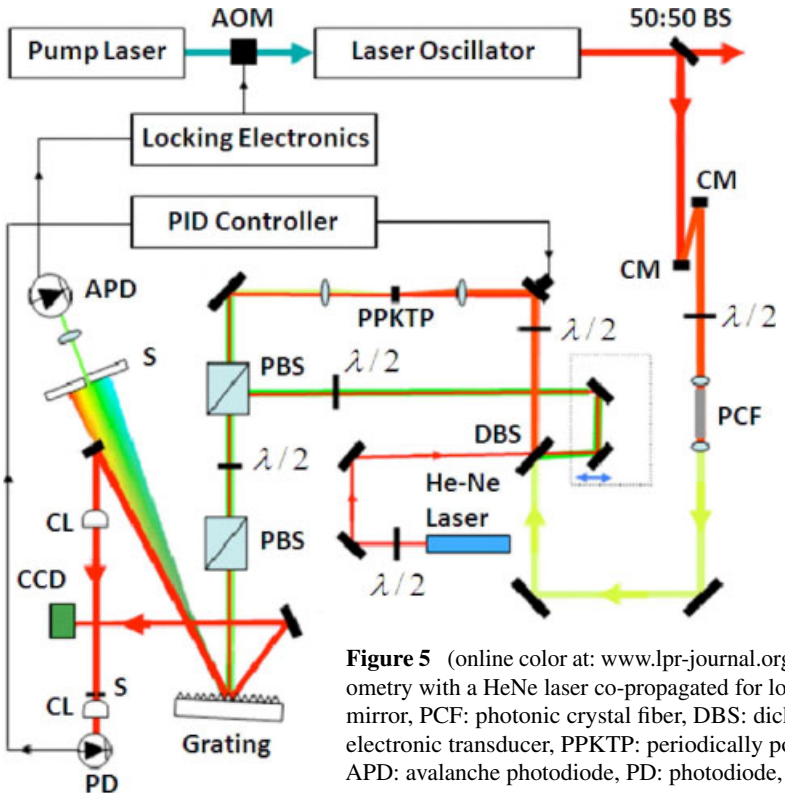

Figure 5 (online color at: www.lpr-journal.org) Interferometer for f-to-$2f$ self-referencing interferometry with a HeNe laser co-propagated for locking the path length. BS: beamsplitter, CM: chirped-mirror, PCF: photonic crystal fiber, DBS: dichroic beamsplitter, $\lambda/2$: half-waveplate, PZT: piezo-electronic transducer, PPKTP: periodically poled KTP, PBS: polarizing beamsplitter cube, S: slit, APD: avalanche photodiode, PD: photodiode, CL: cylindrical mirror, CCD: camera.

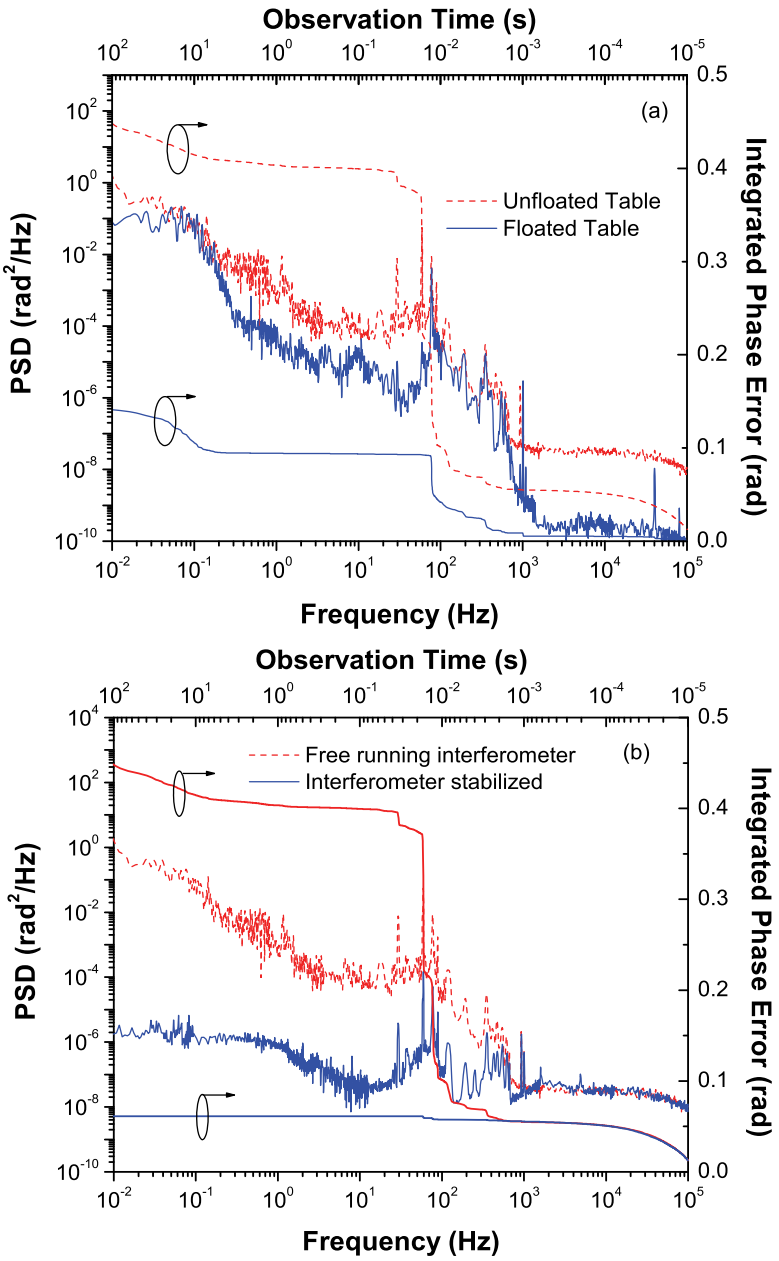

Figure 6 (online color at: www.lpr-journal.org) Comparison of the phase noises of the f-to-$2f$ interferometer between the free running and the stabilized mode. Top: the power spectrum of the interferometer phase noise and the integrated phase error when the optical table was floated and unfloated. Bottom: the power spectrum of the interferometer phase noise and the integrated phase error for the locked and unlocked conditions.

and a servo loop. In addition, the interference signal could be used to investigate the noise dynamics of the interferometer.

Locking the path length greatly reduced the path-length variation and provided more CE-phase stable pulses. The accumulated phase noise is shown in Fig. 6. The phase noise was investigated by sending the photodiode signal to a dynamic signal analyzer and measuring the noise across several frequency spans. The top figure shows the increased stability for floating and unfloating the optical table on which the interferometer was placed. In the bottom figure, the difference between the unlocked and locked interferometer situations is shown. Locking the interferometer greatly reduced the phase noise for frequencies less than ~ 1 kHz. The low-frequency noise was reduced by several orders of magnitude, which greatly improved the CE-phase locking. Consequently, the fast jitter (>3 Hz) of the CE-phase drift of the amplified laser pulses was reduced by over 40%, showing the increase in CE-phase stability.

3.4. Comparison of three types of oscillators

Of course, the type of oscillator and CE-phase stabilization system used is also an important point when discussing stability and ease of use. For octave-spanning lasers, self-phase modulation in the Ti:sapphire crystal is used to generate the broad spectrum [40]. The advantage over other

oscillator designs is that the entire laser output can be used for seeding an amplifier or for other experiments. Also, shorter pulses can usually be produced since the spectrum is so broad. For such a laser, however, the crystal can easily be damaged. Creating the extra frequency components beyond the gain spectrum of Ti:sapphire requires a high intensity in the laser crystal. Also, the alignment of the laser cavity is more difficult than for conventional Ti:sapphire laser oscillators

For conventional Ti:sapphire oscillators, the spectrum is narrower than that of octave-spanning lasers, but the intensity in the laser crystal is lower and the alignment of the cavity is simpler. However, in order to stabilize the CE phase, the spectrum must be broadened to obtain the offset frequency. The advantage is the ease of use of the system. As was said before, the disadvantages in this situation are the path-length drift in the f-to-$2f$, amplitude/phase coupling in the PCF, and a portion of the laser output must be split off to be focused in the PCF.

A compromise exists when the laser output from a broadband Ti:sapphire oscillator is focused into a nonlinear crystal, in which spectral broadening and DFG occur. These processes provide access to the offset frequency. The advantages are that the majority of the laser output would be available and a collinear interferometer could be used to obtain the offset frequency [41]. The disadvantage, though, is the pulse quality from the laser. Pre- and post-pulses exist in the output temporal profile, which can be detrimental to experiments. Also, a somewhat higher intensity must be maintained in the laser crystal for some spectral broadening.

4. CE-phase stabilization and control of amplified laser pulses

The pulse energy of typical Ti:sapphire laser oscillators is on the nJ level, which is not enough for studying the majority of high-field physical processes sensitive to the CE phase, such as ATI [42]. Therefore, the oscillator pulses must undergo amplification to reach higher energies. The most common method for obtaining high-energy pulses is to stretch the pulses in time, amplify them, and then temporally compress them. This scheme is called chirped-pulse amplification (CPA) and is a well-established technology [43–45]. However, in order to obtain high-energy CE-phase stable pulses, any drift introduced during the amplification process must be corrected.

Early investigations of amplifying CE-phase stable pulses focused on identifying and quantifying sources of phase drift [30, 46]. The measurement technique used was called Fourier-transform spectral interferometery (FTSI), whereby the amplified pulses were spectrally broadened over an octave using a nonlinear process, the second harmonic of the long-wavelength components was taken, and the second harmonic and fundamental were overlapped and interfered [47]. Note that this is the method used by almost all groups to measure the CE-phase stability of amplified laser pulses.

It was determined that the CPA process only caused a small, slow drift of the CE phase, which could be precompensated using the oscillator CE-phase locking servo [48–50]. However, the early CE-phase stable amplifiers used glass blocks in the stretchers and prisms in the compressors. These amplifiers could not be scaled up to the multi-mJ level due to the low damage threshold and nonlinear effects of the material in the stretchers and compressors. Therefore, grating-based CPAs were desired as the gratings could handle the higher laser energies. It was initially believed that the CE phase would experience more fluctuation with the grating-based stretchers and compressors; however, it was shown that high-energy CE-phase stable pulses could be obtained from a grating-based CPA [51, 52].

4.1. CE-phase shift caused by grating pairs

It was soon shown that the grating separation could be manipulated to stabilize the CE phase of amplified laser pulses [53]. The scheme for phase control by using the grating separation is illustrated in Fig. 7 [54]. In the figure, two stretcher arrangements are shown. The top figure shows a mirror-based stretcher, which is the one used in the experiments in this paper, and the bottom figure shows a lens-based stretcher. The analysis is also valid for grating compressors.

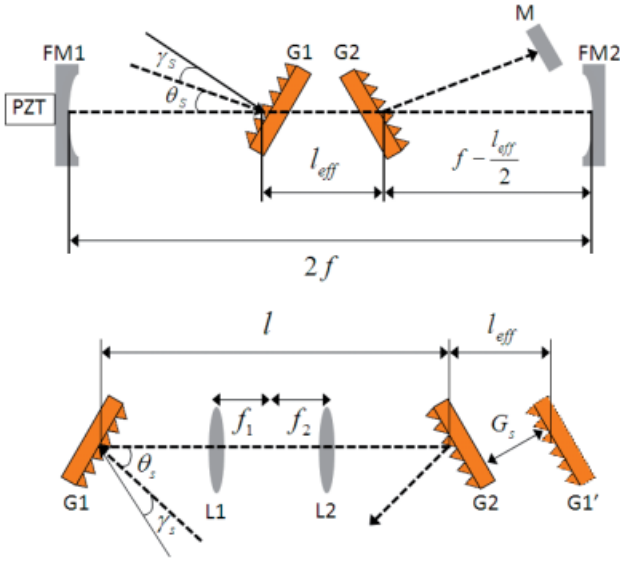

Figure 7 (online color at: www.lpr-journal.org) Grating stretcher. The top figure uses mirrors to form the telescope and the bottom figure uses lenses to form the telescope. In both figures: G1 and G2 are the gratings, FM1 and FM2 are the focusing mirrors, PZT: piezoelectronic transducer, γ_s: the incidence angle on the first grating, θ_s: the angle between the diffracted beam and incident beam, $l_{\rm eff}$: the effective grating separation, G1': the image of G1 in the bottom figure.

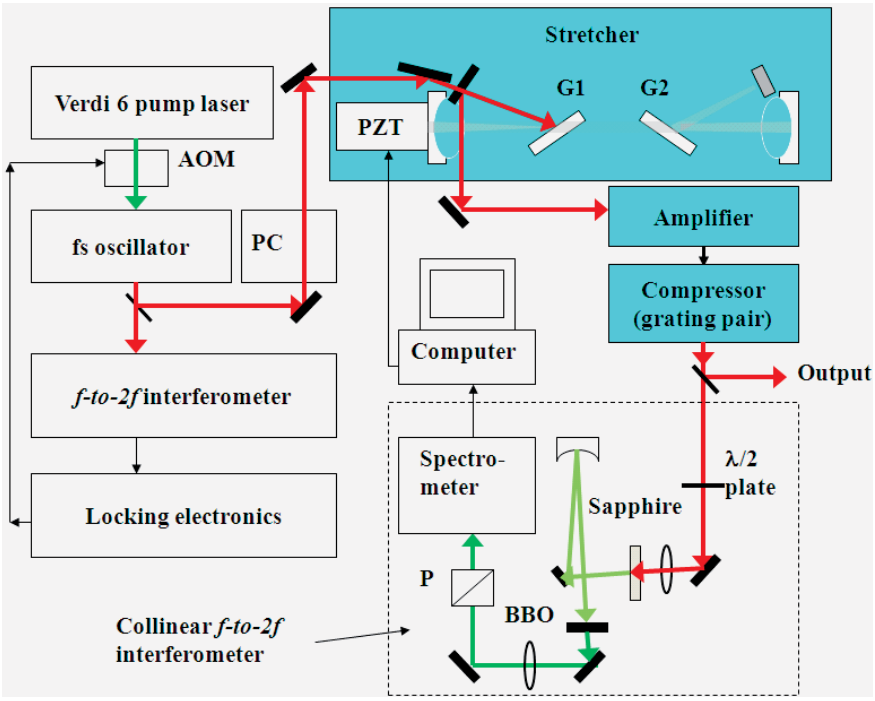

Figure 8 (online color at: www.lpr-journal.org) Kansas Light Source laser system for testing the effects of the grating separation of the stretcher on the CE-phase stability. G1 and G2 are the gratings. M1 is one of the telescope mirrors driven by a piezoelectronic transducer (PZT). The oscillator CE offset frequency f_0 is stabilized by feedback controlling the acousto-optic modulator (AOM). Pulses with the same CE phase are selected by the Pockels cell (PC) are sent to the chirped pulses amplifier.

Using the method of [53], it was shown that the CE-phase shift was given by:

$$\begin{aligned}\Delta\varphi_{\mathrm{CE}} &= \omega_0\tau(\omega_0) - \varphi'(\omega_0) \\ &= 4\pi\left(\frac{G_{\mathrm{S}}}{d_{\mathrm{S}}}\right)\tan[\gamma_{\mathrm{S}} - \theta_{\mathrm{S}}(\omega)]\,, \end{aligned} \tag{7}$$

where $\omega_0\tau(\omega_0)$ is the group delay, $\varphi'(\omega_0)$ is the phase delay, G_{S} is the effective perpendicular distance between gratings, d_{S} is the grating constant, γ_{S} is the angle of incidence, and $\theta_{\mathrm{S}}(\omega)$ is the diffraction angle. By making the substitution $G_{\mathrm{S}} = -l_{\mathrm{eff}}\cos(\gamma_{\mathrm{S}} - \theta_{\mathrm{S}})$, where l_{eff} is the effective linear distance between the gratings, the CE-phase shift becomes:

$$\Delta\varphi_{\mathrm{CE}} = -4\pi\left(\frac{\Delta l_{\mathrm{eff}}}{d_{\mathrm{S}}}\right)\sin(\gamma_{\mathrm{S}} - \theta_{\mathrm{S}})\,. \tag{8}$$

Considering the incident angle is close to the Littrow angle and the grating constant is of the order of a wavelength, the CE-phase shift becomes approximately:

$$\frac{\Delta\varphi_{\mathrm{CE}}}{\Delta l_{\mathrm{eff}}} = 2\pi\frac{\lambda}{d_{\mathrm{S}}^2} \approx \frac{2\pi}{\lambda}. \quad . \tag{9}$$

Thus, Eq. (9) shows that a change in the grating separation comparable to a wavelength will yield a large change in CE phase. Eqs. (8) and (9) also show how the CE phase can be controlled and stabilized by changing the grating separation.

The experimental setup used in determining the effect of the grating separation on the CE phase is shown in Fig. 8. One of the mirrors in the stretcher was placed in a PZT-controlled mount. CE-phase stable pulses from the oscillator were sent to the CPA system. An f-to-$2f$ interferometer, spectrometer, and computer measured the spectral interferometry signal from which the CE phase was extracted. In the f-to-$2f$, the laser was focused into a sapphire plate for spectral broadening and then the infrared components were frequency doubled by a BBO crystal. Finally, a polarizer was used to select a common polarization and the beam was sent to a spectrometer. The resulting interferogram was analyzed by a computer to retrieve the CE-phase drift. For each data point, 50 laser shots were integrated. In the experiment, a 60-V sinusoidal voltage was applied to the PZT and observed. As a comparison, a DC voltage was applied to the PZT. The results are shown in Fig. 9 [54]. It was determined from the measurement that a 1-μm change in grating separation introduced a 3.7 ± 1.2 rad phase shift.

4.2. Stabilizing the CE phase by controlling gratings in stretchers

The grating separation was used as a feedback control to stabilize the CE-phase drift of the amplified pulses. This is shown in Fig. 10, where the CE-phase error was kept to 160 mrad rms over 800 s. 50 laser shots were integrated for each data point. This was the standard experimental procedure for all CE-phase measurements in the KLS laboratory. The bottom plot shows the PZT movement during the same period. The concept of controlling the stabilized CE phase is illustrated in Fig. 11 [55]. The experimental setup used in [55] was the same as in [54], which was a 2.5 mJ, 35 fs Ti:sapphire multipass amplifier [56]. In Fig. 11, the grating separation was precisely controlled to scan the phase over a range of 2π. In the experiment, the setpoint for lock-

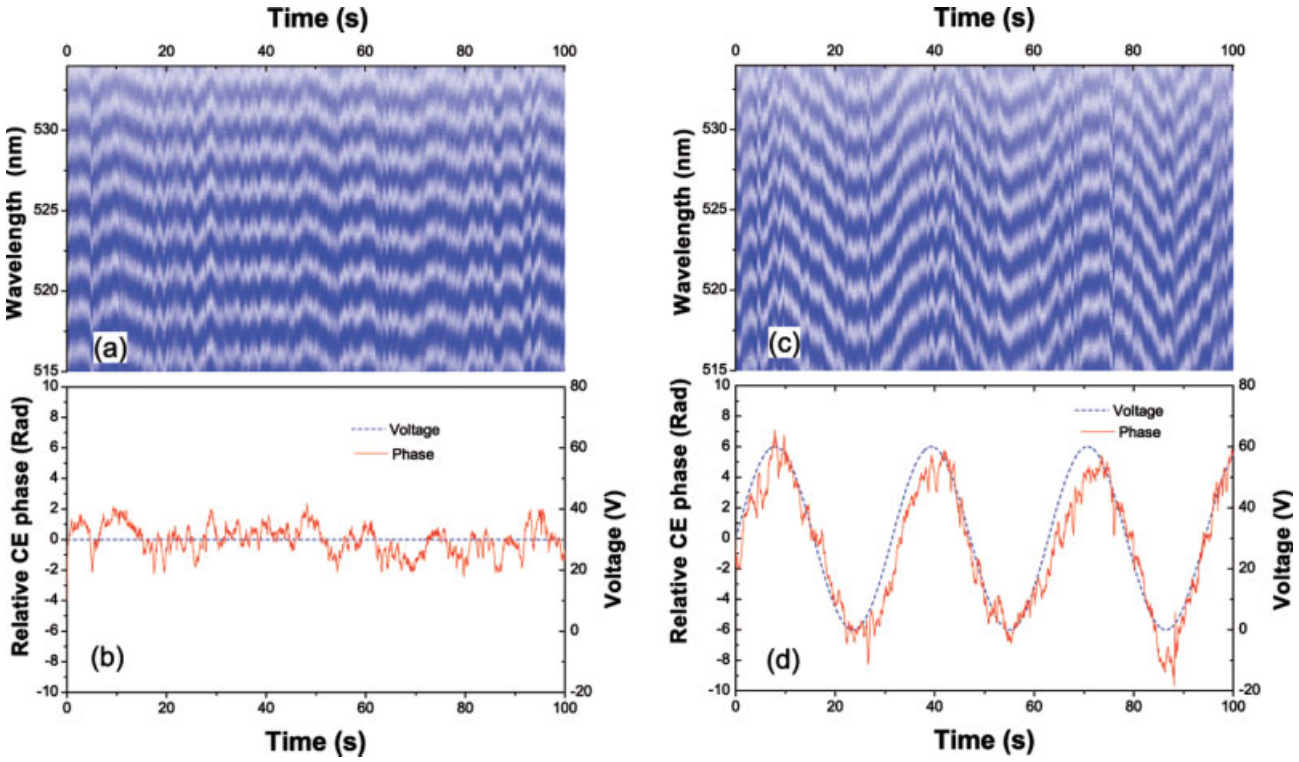

Figure 9 (online color at: www.lpr-journal.org) Dependence of the CE phase of the amplified pulses on the grating separation. (a) Fringe pattern and (b) corresponding relative CE phase obtained with a 30-V DC voltage applied to the PZT. (c) Fringe pattern and (d) corresponding relative CE phase obtained with a 60-V sinusoidal voltage applied to the PZT, which caused the PZT to move 3.6 µm.

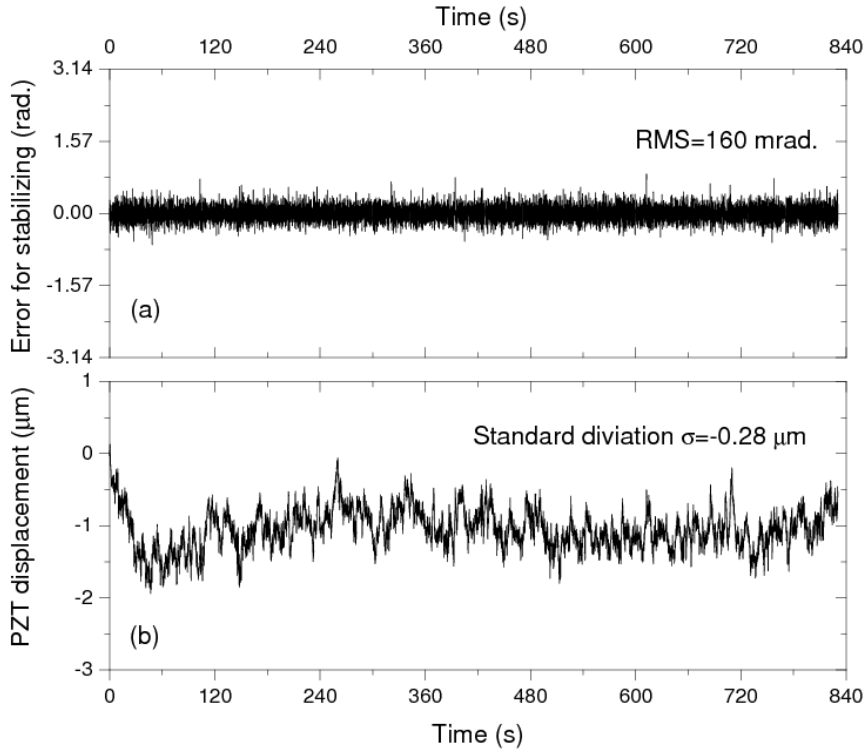

Figure 10 (a) The error signal for the slow feedback stabilization, (b) the displacement of the PZT when the setpoint was shifted.

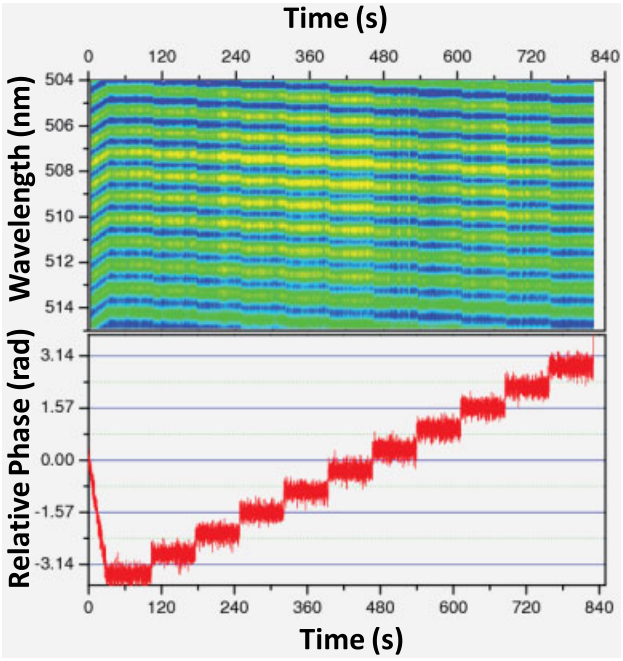

Figure 11 (online color at: www.lpr-journal.org) Precisely controlling the CE phase in amplified pulses. Top: the temporal evolution of interference fringes measured with a collinear f-to-2f interferometer. Bottom: the swept CE phase.

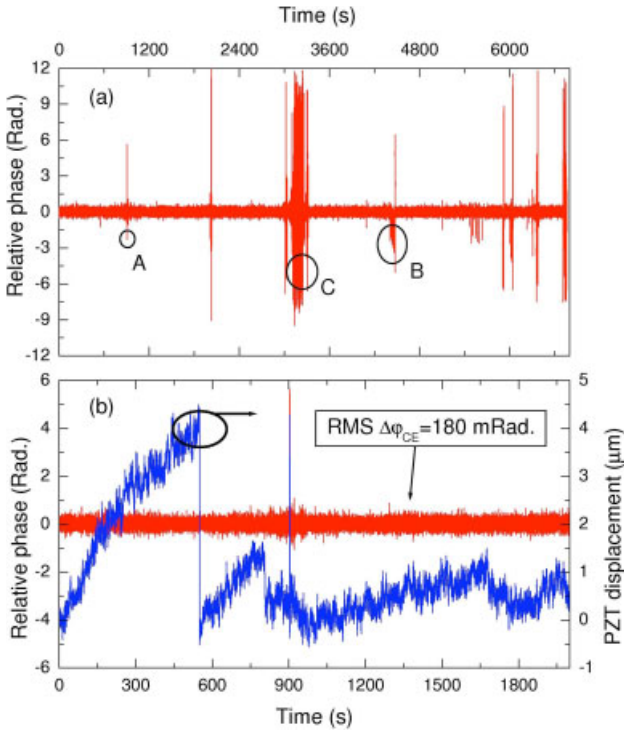

Figure 12 (online color at: www.lpr-journal.org) (a) Temporal evolution of relative CE phase. A, B, and C represent the three kinds of error spikes, respectively. (b) the relative CE phase and the displacement of PZT in the first 32 min in (a).

ing the phase was changed from –1.1π to 0.9π in steps of 0.2π. The relative CE phase was kept at each setpoint for 1 minute and then moved to the next setpoint. During the process, the phase error was smoothly locked to an average of 161 mrad rms, which showed how well the gratings could stabilize the CE phase and change the CE phase simultaneously. Note that in the algorithm used, the first detected fringe pattern was phase zero. Therefore, the CE phase was changed relative to the first detected phase, which had an unknown value.

In Fig. 12, the long-term stability of the grating-based CE phase control is shown along with a description of three kinds of errors typically experienced by the system. In the experiment, the CE phase was locked over 110 min, except at point C in the top plot, where the oscillator CE-phase stabilization stopped working and needed to be reset. Once the oscillator CE-phase stabilization was re-established, the amplifier locking started correcting the slow CE-phase drift. At point A in the top plot, a sharp error spike occurred, which was due to a mechanical disturbance such as touching the optical table, and was quickly corrected within three seconds by the locking system. However, at point B, another disturbance occurred, which caused the CE-phase error to move out of the range of the PZT. However, as the error came within the range of the PZT, the CE phase was relocked within 45 s. In the bottom plot, the CE phase was locked for over 32 min with an rms error of 180 mrad. Also, the figure shows how the PZT moved with the CE-phase error. This is shown near the 900 s mark when a spike occurred in the CE-phase error and the PZT moved with it to correct the error.

Thus, it was shown that the grating separation could be used to stabilize the CE-phase drift of the amplified pulses and to precisely control the phase for experiments. In the introduction to this section, it was noted that groups used the error signal of the CE-phase drift of the amplified pulses to precompensate the drift using the oscillator locking electronics. An added benefit of using the grating separation as a feedback mechanism is that the oscillator locking is unburdened of the extra control, making the oscillator locking more stable.

4.3. Stabilizing the CE phase by controlling gratings in compressors

Similarly, the grating separation in a compressor can also be used to control and stabilize the CE phase. The size of the optic to be used as a control mechanism should be considered when choosing to use either the stretcher or compressor. A large optic, such as a large mirror in the stretcher, would be harder to move using a PZT than a smaller optic. Also, a larger bandwidth of CE-phase noise could be suppressed with a smaller optic.

The effects of controlling the grating separation in a compressor arrangement were investigated [57]. The exper-

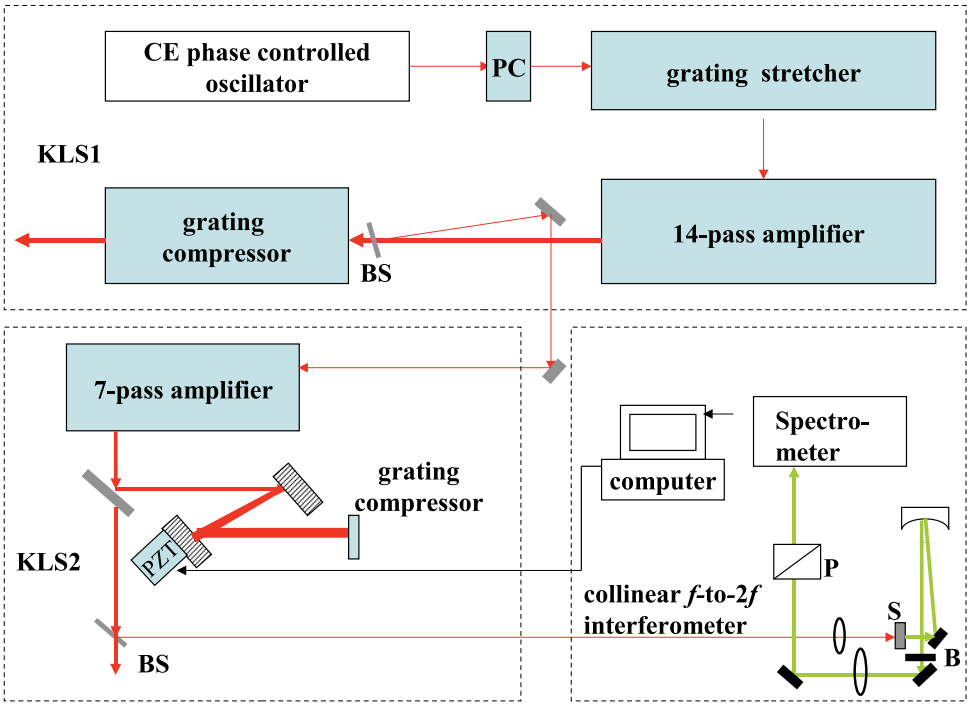

Figure 13 (online color at: www.lpr-journal.org) Experimental setup for controlling the CE phase of the amplified laser pulses. PC: Pockels cell; PZT: piezoelectric transducer; BS: beamsplitter; S: sapphire plate; B: frequency-doubling crystal; P: polarizer.

imental setup used to investigate the compressor control is shown in Fig. 13. Controlling the compressor grating separation was found to stabilize the CE phase to 230 mrad rms over 270 s, which was nearly the same as the stretcher grating performance. Fig. 14 shows the performance of the compressor grating separation control. The top plot shows the difference between the situation where the feedback control was turned on and when it was inactive. The bottom plot shows the fast Fourier transform of the phase drift. The plot shows how the feedback control corrects CE-phase error under 4 Hz. This is expected since the drift of CE-phase-stable pulses through an amplifier is slow, since the oscillator stabilization corrects the majority of the fast drift. However, as in [39], locking the path-length difference in the oscillator CE-phase stabilization interferometer will reduce the fast noise (>3 Hz) by over 40%, which can improve the overall CE-phase-locking quality of the system.

5. Power locking and carrier-envelope phase stability

5.1. Power locking of CPA

In [37], it was shown that power fluctuations of the oscillator would affect the accuracy of the CE-phase stabilization by causing a nonlinear amplitude-to-phase coupling in microstructure fiber. Similarly, when obtaining the CE-phase error of the amplified laser pulses, a nonlinear process is

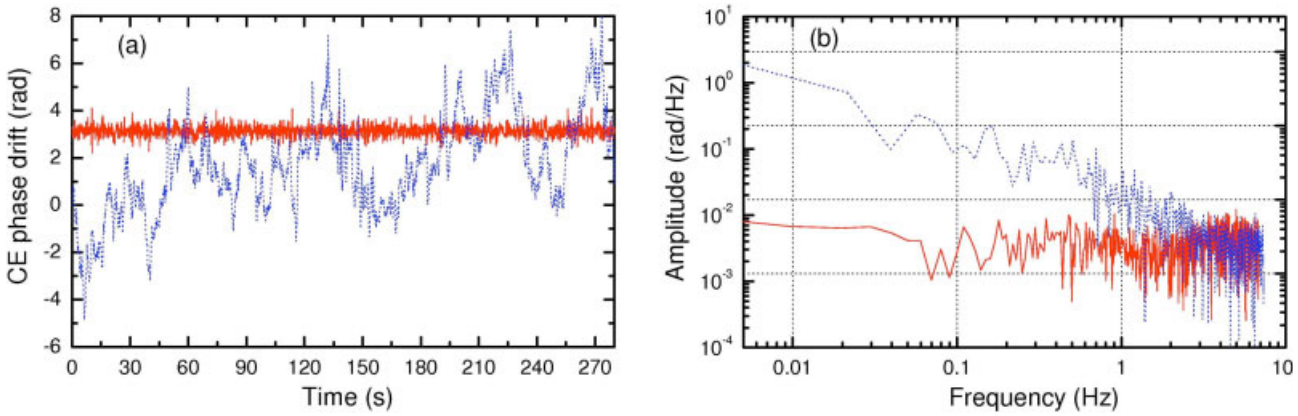

Figure 14 (online color at: www.lpr-journal.org) (a) The evolution of the freely drifting (dotted line) and stabilized (solid line) CE phase. (b) The fast Fourier transform of the CE-phase drift under the free-running (dotted line) and stabilized conditions (solid line).

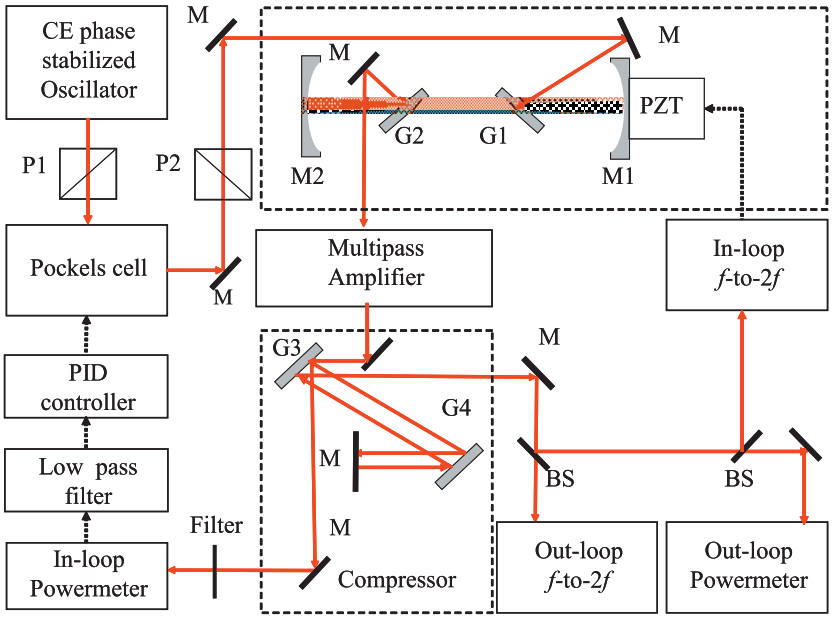

Figure 15 (online color at: www.lpr-journal.org) The Kansas Light Source (KLS) laser-intensity-stabilization system. The in-loop powermeter was put in the path of the zero-order diffraction beam and sent the power signal to the PID controller. By using feedback control, the PID varied the voltage applied on the Pockels cell, which in turn changed the polarization of the output from the oscillator and stabilized the laser intensity. Red arrows are the laser paths and dashed arrows represent electronic circuits.

used, such as self-phase modulation, to broaden the pulse spectrum over an octave in order to perform f-to-$2f$ interferometry [47]. Usually, the Ti:sapphire laser is focused into a bulk material, such as sapphire, to generate the octave-spanning spectrum. Therefore, the nonlinear process should be susceptible to intensity fluctuations that would also affect the measured CE phase.

The energy fluctuation of typical diode-pumped kilohertz femtosecond laser systems is around 1.5% RMS, even when placed in a well-controlled environment and allowed hours of warm-up time. In order to increase the energy stability of those systems, a power-locking system was developed, which measured the power after the amplifier and feedback controlled the Pockels cell pulse-selection amplitude. An energy stability of 0.3% RMS was observed using this method [58]. In order to investigate the effects of energy fluctuation on the CE phase, an out-of-loop f-to-$2f$ was constructed, which would measure the CE-phase stability of the amplified pulses. The experimental setup is shown in Fig. 15. Basically, the in-loop f-to-$2f$ measured and stabilized the CE-phase drift of the amplified pulses, while the out-of-loop f-to-$2f$ only measured the CE-phase drift. The measurement was done for both the power-locked and unlocked situations. The results are shown in Fig. 16. It is clearly shown that the energy stability of the amplified laser pulses is important for CE-phase measurement accuracy.

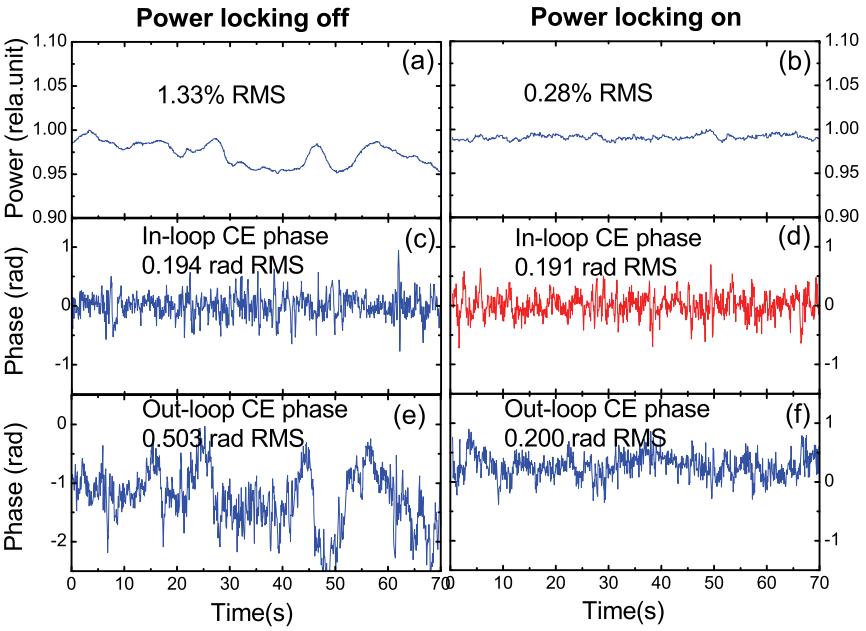

Figure 16 (online color at: www.lpr-journal.org) The left column and right column were the measurement of laser power and CE-phase stability with and without power locking. (a) and (b) show normalized power. After stabilization, the power fluctuation had decreased to one fifth of its usual value; (c) and (d) are in-loop CE phase; (e) and (f) are out-of-loop CE phase.

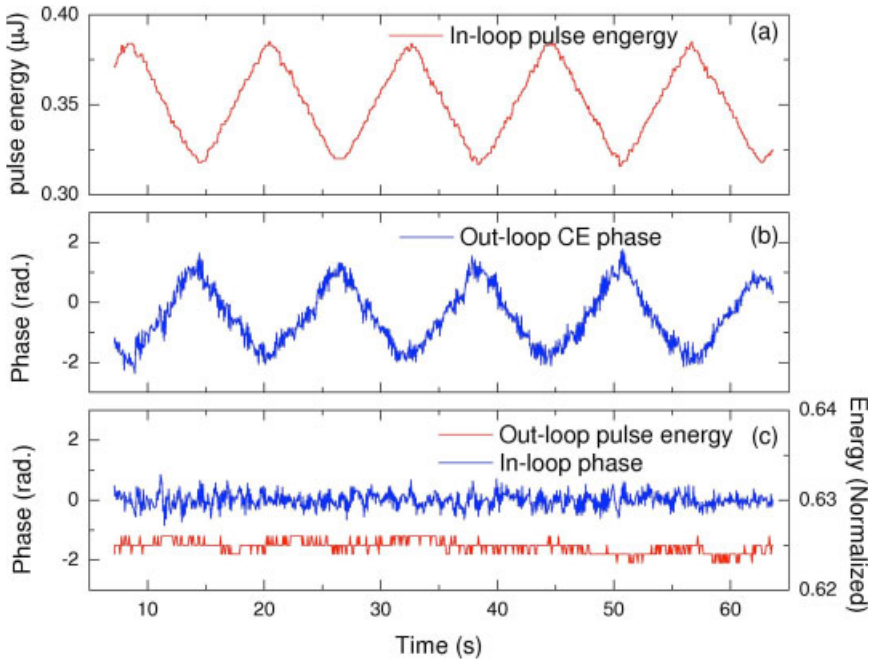

Figure 17 (online color at: www.lpr-journal.org) Temporal evolution of measured phase and laser energy. (a) Modulated in-loop pulse energy, (b) measured out-of-loop phase, and (c) the in-loop phase and out-of-loop energy.

In order to measure the effect of a 1% energy change on the measurement accuracy of the f-to-$2f$ interferometer, the power of the laser system was locked and the in-loop f-to-$2f$ was used to lock the phase. However, the laser energy input to the in-loop f-to-$2f$ was modulated. The out-of-loop f-to-$2f$ was used to measure the phase [59]. Fig. 17 shows the results of the experiment. It was determined that a 1% energy change led to a 160-mrad CE-phase error, which is quite large and indicates the need for good laser-energy stability.

The energy dependence of the CE-phase measurement can be understood by looking at the frequency-domain representation of the spectral interferogram that is given:

$$S(\omega) = I_{\mathrm{WL}}(\omega) + I_{\mathrm{SHG}}(\omega) + 2\sqrt{I_{\mathrm{WL}}(\omega) I_{\mathrm{SHG}}(\omega)} \times \cos\left[\varphi_{\mathrm{SHG}}(\omega) - \varphi_{\mathrm{WL}}(\omega) - \omega\tau_0 + \varphi_{\mathrm{CE}}^{\mathrm{WL}}\right], \tag{10}$$

where τ_0 is the delay between the fundamental and frequency-doubled pulses, $\varphi_{\mathrm{SHG}}(\omega)$ is the spectral phase of the frequency doubled pulse, and $\varphi_{\mathrm{WL}}(\omega)$ is the spectral phase of the fundamental pulse. The total phase, which is in the argument of the cosine, is set to zero during the CE-phase stabilization process. However, the terms in the total phase are intensity dependent, which has been explained by a simple two-step model [60]. Then, if the total phase is set to zero and there is energy fluctuation, the CE phase will still suffer an error, which can be written as:

$$\Delta\varphi_{\mathrm{CE}}^{\mathrm{err}} = -\Delta\left[\varphi_{\mathrm{SHG}}(\omega) - \varphi_{\mathrm{WL}}(\omega) - \omega\tau_0 + \delta\varphi_{\mathrm{CE}}\right], \tag{11}$$

whereas the CE-phase measured by the interferometer would be given by:

$$\Delta\varphi_{\mathrm{CE}} = \Delta\Phi(\omega) - \Delta\left[\varphi_{\mathrm{SHG}}(\omega) - \varphi_{\mathrm{WL}}(\omega) - \omega\tau_0 + \delta\varphi_{\mathrm{CE}}\right], \tag{12}$$

where $\Delta\Phi(\omega)$ is the total phase and is set to zero during the CE-phase stabilization.

5.2. The effects of hollow-core fiber

The aforementioned results were obtained with ~ 35 fs pulses from the laser amplifier. However, for ultrafast science, few-cycle pulses are desired. The usual method for generating short pulses is to use a hollow-core fiber chirped-mirror compressor. The fiber, though, would be subject to beam-pointing fluctuations, which in turn would lead to energy fluctuations of the few-cycle pulses. Also, laser-energy fluctuations before the fiber would exacerbate the problem.

These issues were addressed in [14], where the CE-phase stability of the few-cycle pulses were measured in an out-of-loop f-to-$2f$ [14]. In the experiment, the CE phase of the pulses before the fiber was locked and the CE-phase stability of the few-cycle pulses was measured for the power-locked and unlocked situations. It was found that the CE-phase stability of the few-cycle pulses was 370 mrad rms with an in-loop stability of 180 mrad rms when the power was locked. Alternately, when the power was unlocked, the CE-phase stability of the few-cycle pulses was 567 mrad rms with an in-loop stability of 195 mrad rms. This work again showed the importance of power stability, especially for measuring few-cycle pulse stability.

6. Double optical gating with CE phase-stabilized pulses

6.1. Single isolated attosecond pulses

Recently, single attosecond pulse production has become a hot topic in the ultrafast optics field [61]. Such extremely short XUV pulses are powerful tools for studying electron dynamics in atoms and molecules [62]. This new light source is based on high-order harmonic generation (HHG), which is a nonperturbative nonlinear optic process discovered around 1987–1988 [63]. When a linearly polarized, short pulse laser beam interacts with noble gases, odd harmonics of the fundamental frequency, up to hundreds in order, emerge in the output beam. According to the semiclassical model, when the laser intensity approaches a fraction of one atomic unit (3.55×10^{16} W/cm^2), an electron wavepacket first moves away from the nucleus of the target atom through tunneling, then is driven back. Finally, it recombines with the parent ion with the emission of a coherent burst of X-rays [64, 65]. These three steps occur within one laser cycle. When all electrons released near one peak of a laser cycle are considered, the emitted photons form an attosecond pulse. Since there are two field maxima in one laser cycle, two attosecond pulses are generated by those electrons that take the "short trajectories". For a laser pulse that contains many cycles, an attosecond pulse train is produced [66]. The pulse train corresponds to discrete harmonic peaks in the frequency domain, which is the high-harmonic spectrum.

When the duration of the laser pulse approaches one cycle, the harmonic peaks in the cutoff region merge into a continuum, which has been filtered out to produce single isolated attosecond pulses [67]. The shortest pulse generated so far is 80 attoseconds. Single isolated attosecond pulses can also be extracted by a scheme called polarization gating [68, 69]. It uses a laser field with a rapidly changing ellipticity. Since XUV attosecond pulses can only be efficiently generated with linearly polarized driving fields, a single attosecond pulse is emitted if the laser field is linearly polarized in only a short time range and elliptically polarized in the other portion of the driving pulse. The time range over which the attosecond pulse is generated is called the polarization gate. This scheme was demonstrated with 5-fs lasers [70]. However, it is still a technical challenge to reproduce daily laser pulses with one- to two-cycle duration. We developed a double optical gating (DOG) technique for generating single isolated attosecond pulses with multicycle pump lasers [5].

6.2. Double optical gating

The double optical gating combines polarization gating with a weak second-harmonic field. The polarization gating field can be created by adding two circularly polarized pulses together. The field synthesis can be done with birefringence optics. Details of the experimental setup can be found in [6]. This method allows the linear portion of the ellipticity dependent pulse to be a full optical cycle of the input pulse as compared to the half-optical-cycle requirements of polarization gating alone.

The laser field for the double optical gating can be resolved into a driving field and gating field, $\mathbf{E}(t) = E_{\rm drive}(t)\hat{i} + E_{\rm gate}(t)\hat{j}$, where $\hat{i}$ and $\hat{j}$ are the unit vectors in the x and y directions, respectively. The driving field generates the attosecond pulses, whereas the gating field suppresses attosecond emissions except the one in the middle of the laser pulse. The driving field is

$$\begin{aligned} E_{\rm drive}(t) = & E_0 \Bigg[\left(\mathrm{e}^{-2\ln 2 \frac{(t+T_{\rm d}/2)^2}{\tau_{\rm p}^2}} + \mathrm{e}^{-2\ln 2 \frac{(t-T_{\rm d}/2)^2}{\tau_{\rm p}^2}} \right) \\ & \times \cos(\omega_0 t + \varphi_{\rm CE}) \\ & + a_{\omega,2\omega} \left(2\,\mathrm{e}^{-2\ln 2 \left(\frac{T_{\rm d}/2}{\tau_{\rm p}}\right)^2} \right) \mathrm{e}^{-2\ln 2 \frac{t^2}{\tau_{2\omega}^2}} \\ & \times \cos(2\omega_0 t + 2\varphi_{\rm CE} + \varphi_{\omega,2\omega}) \Bigg] \end{aligned} \quad (13)$$

and the gating field is

$$\begin{aligned} & E_{\rm gate}(t) = \\ & E_0 \left(\mathrm{e}^{-2\ln 2 \frac{(t+T_{\rm d}/2-T_\omega/4)^2}{\tau_{\rm p}^2}} - \mathrm{e}^{-2\ln 2 \frac{(t-T_{\rm d}/2-T_\omega/4)^2}{\tau_{\rm p}^2}} \right) \\ & \times \sin(\omega_0 t + \varphi_{\rm CE}) \,, \end{aligned} \quad (14)$$

where E_0 is the amplitude of the circularly polarized fundamental laser field with a carrier frequency ω_0 and a pulse duration $\tau_{\rm p}$. The delay, $T_0/4$, between the gating and the driving fields is introduced by a quarter-wave plate for creating the circular light. $\varphi_{\rm CE}$ is the carrier-envelope phase of the fundamental laser fields. The carrier-envelope phase of the second-harmonic field is $2\varphi_{\rm CE}$. $a_{\omega,2\omega}$ is the ratio of the amplitudes between the second-harmonic field and the driving field at the center of the polarization gate ($t = 0$). The relative phase delay between the two fields is$\varphi_{\omega,2\omega}$ when $\varphi_{\rm CE} = 0$.

6.3. The effects of CE phase on the gated XUV spectra

Since the effective generation portion of the input pulse is a single cycle or less, the CE-phase dependence exhibits very strong features. Fig. 18 shows the field within the linear portion of the ellipticity dependent pulse. The vertical lines indicate the "gate width" which is the linear portion actually responsible for generating a single pulse. The figure also shows that as the CE phase of the input pulse changes, the attosecond pulses that are generated can change in intensity and be either a single pulse or a set of two pulses. Due to

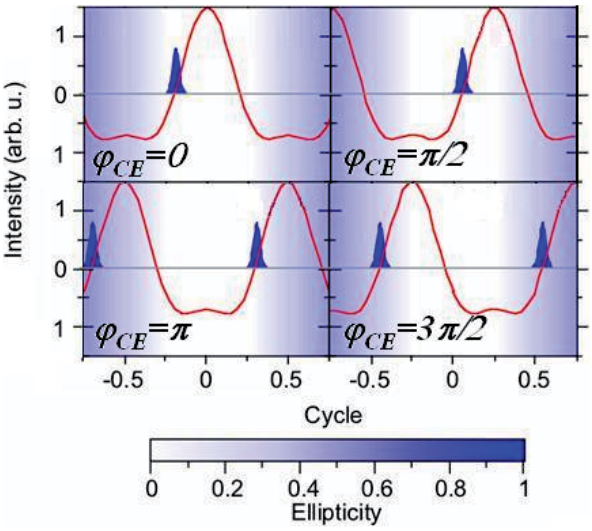

Figure 18 (online color at: www.lpr-journal.org) The semiclassical prediction of the waveform within the gate width when the CE phase is scanned. The color indicates the strength of the ellipticity. The blue peaks are the attosecond extreme ultraviolet bursts generated by the laser field and the red line indicates the field itself.

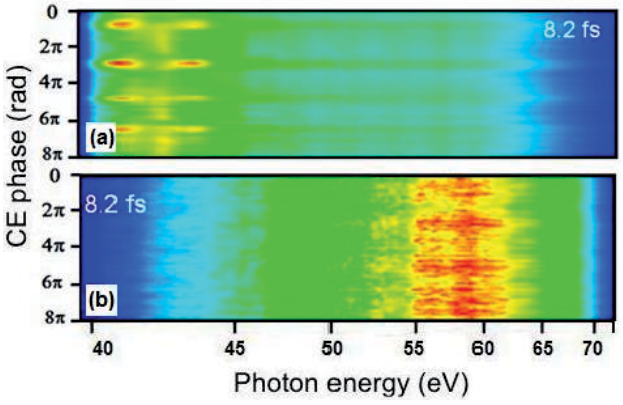

Figure 19 (online color at: www.lpr-journal.org) Extreme ultraviolet spectra as a function of the laser field CE phase. The conditions are for 8.2-fs pulses on (a) an argon gas target and (b) a neon gas target.

the asymmetry of the driving field, the dependence of the spectra on the CE phase has a 2π periodicity.

The top plot in Fig. 19 shows the harmonic spectrum as a function of the input pulse CE phase for an argon gas target with 8-fs pulses. The CE phase was stabilized and varied by controlling the grating separations in the pulses stretcher. The spectrum switches between a broad continuum and several discrete orders with a 2π periodicity in agreement with Fig. 18. The bottom plot in Fig. 19 shows the same scan but with neon gas as the target. Since the ellipticity dependence on the harmonic-generation process

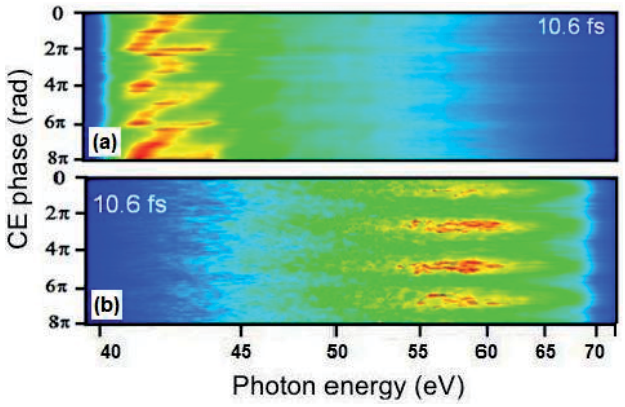

Figure 20 (online color at: www.lpr-journal.org) Extreme-ultraviolet spectra as a function of the laser field CE phase. The conditions are for 10.6-fs pulses on (a) an argon gas target and (b) a neon gas target.

is stronger for higher harmonics, the portion of the pulse that generates high-order harmonics is effectively reduced. This results in a 2π periodicity but without the possibility of two attosecond pulses being generated. This is shown as a spectrum with a strong modulation in the intensity of the continuum but no discrete orders.

Due to the reduced target depletion with intensity of DOG, input pulses as long as 12 fs have been shown to generate broad spectra that can support single attosecond pulses [71]. Fig. 20 shows the harmonic spectrum as a function of the input CE phase for 10-fs pulses in argon and neon gases. The spectra show similar features as compared with the 8-fs results and the 2π periodicity allows for the determination of the absolute CE phase of the input pulse even for such long pulses.

7. Conclusions

In summary, it has been shown that CE-phase technology has improved over the years since CE-phase stabilization of Ti:sapphire laser oscillators and amplifiers was first experimentally realized. Several methods now exist for stabilizing the offset frequency, f_0 of mode-locked laser oscillators, including f-to-$2f$ self-referencing and difference-frequency generation. State-of-the-art methods even include obtaining the offset frequency using intracavity methods [72]. For amplified pulses, stabilization of the CE-phase drift through the CPA was shown to be viable technology by using f-to-$2f$ interferometry of the high-energy pulses and feeding back to either the oscillator stabilization electronics or by changing the grating separation. The grating-based CPA and CE-phase control methods, however, were shown to be a much better technology, as the pulses could be scaled to the multi-mJ level and the CE phase could be precisely controlled. In addition, the effects of laser-energy fluctuation of the CPA on the CE-phase measurement and stabilization

were studied and were found to be significant. The laser energy fluctuation, therefore, should be kept below 1% for reliable CE-phase measurement and stabilization. This was especially evident for short pulse generation using a hollow-core fiber chirped-mirror compressor. Therefore, CE-phase stable and controllable high-energy pulses are now a viable technology for studying ultrafast science.

Challenges do lie ahead for CE-phase-stabilization technology. For example, adaptive pulse shaping is a method where the phase of the laser pulse can be manipulated. If this method is combined with CE-phase stabilization and control, it could allow for the generation of ultrashort pulses with precise control of the absolute phase. Also, by improving the power stability of few-cycle pulses generated from filamentation or hollow-core fiber chirped-mirror compressors, the CE phase of short pulses could be more finely controlled. Finally, the majority of the work with CE-phase stabilization and control of amplified laser pulses has been with multipass Ti:sapphire amplifiers. To date, no group has actively stabilized and controlled the CE phase of regenerative amplifiers. This is also one of the major challenges still facing CE-phase researchers. Thus, there is room to improve in the area of CE-phase stabilization and control of Ti:sapphire laser oscillators and amplifiers.

Acknowledgements The authors would like to thank all of the current and former members of the Kansas Light Source research group for helpful discussions, design of equipment, and further assistance. This work was supported by the Chemical Sciences, Geosciences and Biosciences Division, Office of Basic Energy Sciences, Office of Science, U. S. Department of Energy, by the National Science Foundation under grant No. 0457269, and by the U. S. Army Research Office under grant number W911NF-07-1-0475.

Eric Moon graduated with a B. S. in Physics from Baker University in Baldwin City, KS in 2003. He finished a Ph. D. in Physics at Kansas State University in December 2008. His research was focused on carrier-envelope stabilization of Ti:sapphire lasers and amplifiers. He currently works for Quantronix in East Setauket, NY.

He Wang received his B.S degree in physics from University of Science and Technology of China in 2005. Currently, he is a fourth-year graduate student in the physics department at Kansas State University. His current research is mainly focused on the generation of CE-phase-controllable short pulses with a pulse shaper and their applications.

Steve Gilbertson received the B. S. degree from Kansas State University in 2005. He is currently working toward the Ph. D. degree from Kansas State University, Manhattan, Kansas. His research interests include applications of soft X-ray radiation from high-harmonic generation and attosecond science.

Hiroki Mashiko received the B. S. and M. S. degrees from Tokai University, Department of Physics, Kanagawa, Japan, in 2001 and 2003, respectively. The Ph. D. degree was received from Saitama University, Graduate School of Science and Engineering, Saitama, Japan in 2006. From April 2003–2006, he was a Junior Research Associate at the Institute of Physical and Chemical Research (RIKEN), Laser Technology Laboratory, Japan. From March 2006, he joined as a Post-Doctoral Research Associate at Kansas State University, Department of Physics, USA.

Michael Chini received his B. S. degree in physics from McGill University in 2007. He is currently in the second year of his Ph. D. studies in the physics department at Kansas State University. His current research is mainly focused on single attosecond pulse generation and characterization.

Dr. Zenghu Chang is a professor of physics at Kansas State University. He received his doctorate in Optics at the Xi'an Institute of Optics and Precision Mechanics at the Chinese Academy of Sciences in 1988. He served as an associate professor at this intuition for the next three years before joining the Rutherford Appleton Laboratory in the UK. Dr. Chang moved to the US in 1995 with a position at Washington State University as an adjunct professor and visiting scientist. In 1996 he moved to the University of Michigan as a research fellow and then as an Assistant research scientist. In 2001 he joined the faculty at Kansas State University and in 2006 was appointed full professor in the Department of Physics. Most recently Dr. Chang was awarded a Mercator Professorship, by the German Science Foundation. He now serves as the chair of the attoscience technique

group of the Optical Society of America. His research activities include the area of coherent extreme ultraviolet attosecond sources from high-order harmonic generation.

References

[1] G. G. Paulus, F. Grasbon, H. Walther, P. Villoresi, M. Nisoli, S. Stagira, E. Priori, and S. De Silvestri, Nature (London) **414**, 182 (2001).
[2] C. A. Haworth, L. E. Chipperfield, J. S. Robinson, P. L. Knight, J. P. Marangos, and J. W. G. Tisch, Nature Phys. **3**, 52 (2007).
[3] G. Sansone, C. Vozzi, S. Stagira, M. Pascolini, L. Poletto, P. Villoresi, G. Tondello, S. De Silvestri, and M. Nisoli, Phys. Rev. Lett. **92**, 113904 (2004).
[4] I. J. Sola, E. Mével, L. Elouga, E. Constant, V. Strelkov, L. Poletto, P. Villoresi, E. Benedetti, J. P. Caumes, S. Stagira, C. Vozzi, G. Sansone, and M. Nisoli, Nature Phys. **2**, 319 (2006).
[5] H. Mashiko, S. Gilbertson, C. Li, S. D. Khan, M. M. Shakya, E. Moon, and Z. Chang, Phys. Rev. Lett. **100**, 103906 (2008).
[6] S. Gilbertson, H. Mashiko, C. Li, S. D. Khan, M. M. Shakya, E. Moon, and Z. Chang, Appl. Phys. Lett. **92**, 071109 (2008).
[7] V. Roudnev, B. D. Esry, and I. Ben-Itzhak, Phys. Rev. Lett. **93**, 163601 (2004).
[8] C. Lemell, X.-M. Tong, F. Krausz, and J. Burgdörfer, Phys. Rev. Lett. **90**, 076403 (2003).
[9] M. Kreb, T. Löffler, M. D. Thomson, R. Dörner, H. Gimpel, K. Zrost, T. Ergler, R. Mashammer, U. Morgner, J. Ullrich, and H. G. Roskos, Nature Phys. **2**, 327 (2006).
[10] T. M. Fortier, P. A. Roos, D. J. Jones, S. T. Cundiff, R. D. R. Bhat, and J. E. Sipe, Phys. Rev. Lett. **92**, 147403 (2004).
[11] W.-J. Chen, Z.-M. Hsieh, S. W. Huang, H.-Y. Su, C.-J. Lai, T.-T. Tang, C.-H. Lin, C.-K. Lee, R.-P. Pan, C.-L. Pan, and A. H. Kung, Phys. Rev. Lett. **100**, 163906 (2008).
[12] Femtolasers FEMTOSOURCE™ RAINBOW™ at www.femtolasers.com; Venteon Pulse 1™, www.venteon.com; KM Labs Griffin™, www.kmlabs.com; Menlosystems Octavius™, www.menlosystems.com.
[13] M. Nisoli, S. De Silvestri, O. Svelto, R. Szipöcs, K. Ferencz, Ch. Spielmann, S. Sartania, and F. Krausz, Opt. Lett. **22**, 522 (1997).
[14] H. Mashiko, C. M. Nakamura, C. Li, E. Moon, H. Wang, J. Tackett, and Z. Chang, Appl. Phys. Lett. **90**, 161114 (2007).
[15] J. H. Sung, J. Y. Park, T. Imran, Y. S. Lee, and C. H. Nam, Appl. Phys. B, Laser Opt. **82**, 5 (2006).
[16] A. Couairon, J. Biegert, C. P. Hauri, W. Kornelis, F. W. Helbing, U. Keller, and A. Mysyrowicz, J. Mod. Opt. **53**, 75 (2006).
[17] G. Stibenz, N. Zhavoronkov, and G. Steinmeyer, Opt. Lett. **31**, 274 (2006).
[18] H. Wang, Y. Wu, C. Li, H. Mashiko, S. Gilbertson, and Z. Chang, Opt. Express **16**, 14449 (2008).
[19] A. Poppe, R. Holtzwarth, A. Apolonski, G. Tempea, Ch. Spielmann, and T. W. Hänsch, Appl. Phys. B, Lasers Opt. **72**, 373 (2001).
[20] R. J. Jones and J.-C. Diels, Phys. Rev. Lett. **86**, 3288 (2001).
[21] S. T. Cundiff, J. Phys. D, Appl. Phys. **35** R43 (2002).
[22] J.-C. Diels and W. Rudolph, Ultrashort Sources I: Fundamentals, in: Ultrashort Laser Pulse Phenomena: Fundamentals, Techniques, and Applications on a Femtosecond Time Scale, 2nd ed. (Elsevier, London, 2006), pp. 283–285.
[23] O. D. Mücke, R. Ell, A. Winter, J.-W. Kim, J. R. Birge, L. Matos, and F. X. Kärtner, Opt. Express **13**, 5163 (2005).
[24] L. Xu, Ch. Spielmann, A. Poppe, T. Brabec, F. Krausz, and T. W. Hänsch, Opt. Lett. **21**, 2008 (1996).
[25] H. R. Telle, G. Steinmeyer, A. E. Dunlop, J. Stenger, D. H. Sutter, and U. Keller, Appl. Phys. B, Lasers Opt. **69**, 327 (1999).
[26] J. K. Ranka, R. S. Windeler, and A. J. Stentz, Opt. Lett. **25**, 25 (2000).
[27] A. Apolonski, A. Poppe, G. Tempea, Ch. Spielmann, Th. Udem, R. Holtzwarth, T. W. Hänsch, and F. Krausz, Phys. Rev. Lett. **85**, 740 (2000).
[28] D. J. Jones, S. A. Diddams, J. K. Ranka, A. Stentz, R. S. Windeler, J. L. Hall, and S. T. Cundiff, Science **288**, 635 (2000).
[29] T. Fuji, A. Apolonski, and F. Krausz, Opt. Lett. **29**, 632 (2004).
[30] F. W. Helbing, G. Steinmeyer, J. Stenger, H. R. Telle, and U. Keller, Appl. Phys. B, Lasers Opt. **74**, S35 (2002).
[31] Y. S. Lee, J. H. Sung, C. H. Nam, T. J. Yu, and K.-H. Hong, Opt. Express **13**, 2969 (2005).
[32] J. Ye, S. T. Cundiff, S. Foreman, T. M. Fortier, J. L. Hall, K. W. Holman, D. J. Jones, J. D. Jost, H. C. Kapetyn, K. A. H. V. Leeuwen, L. S. Ma, M. M. Murnane, J. L. Peng, and R. K. Shelton, Appl. Phys. B, Lasers Opt. **74**, S27 (2002).
[33] T. M. Fortier, D. J. Jones, J. Ye, and S. T. Cundiff, IEEE J. Quantum Electron. **9**, 1002 (2003).
[34] S. T. Cundiff, J. Ye, and J. L. Hall, Rev. Sci. Instrum. **72**, 3749 (2001).
[35] F. W. Helbing, G. Steinmeyer, and U. Keller, IEEE J. Quantum Electron. **9**, 1030 (2003).
[36] K. W. Holman, R. J. Jones, A. Marian, S. T. Cundiff, and J. Ye, IEEE J. Quantum Electron. **9**, 1018 (2003).
[37] T. M. Fortier, J. Ye, S. T. Cundiff, and R. S. Windeler, Opt. Lett. **27**, 445 (2002).
[38] T. M. Fortier, D. J. Jones, J. Ye, S. T. Cundiff, and R. S. Windeler, Opt. Lett. **27**, 1436 (2002).
[39] E. Moon, C. Li, Z. Duan, J. Tackett, K. L. Corwin, B. R. Washburn, and Z. Chang, Opt. Express **14**, 9758 (2006).
[40] S. Rausch, T. Binhammer, A. Harth, J. Kim, R. Ell, F. X. Kärtner, and U. Morgner, Opt. Express **16**, 9739 (2008).
[41] T. Fuji, J. Rauschenberger, A. Apolonski, V. S. Yakovlev, G. Tempea, T. Udem, C. Gohle, T. W. Hänsch, W. Lehnert, M. Scherer, and F. Krausz, Opt. Lett. **30**, 332 (2005).
[42] G. G. Paulus, F. Lindner, H. Walther, A. Baltuška, E. Goulielmakis, M. Lezius, and F. Krausz, Phys. Rev. Lett. **91**, 253004 (2003).
[43] A. Rundquist, C. Durfee, Z. Chang, G. Taft, E. Zeek, S. Backus, M. M. Murnane, H. C. Kapetyn, I. Christov, and V. Stoev, Appl. Phys. B, Lasers Opt. **65**, 161 (1997).

[44] J. Zhou, C.-P. Huang, C. Shi, M. M. Murnane, and H. C. Kapetyn, Opt. Lett. **19**, 126 (1994).
[45] D. Strickland and G. Mourou, Opt. Commun. **62**, 419 (1985).
[46] M. Kakehata, Y. Fujihira, H. Takada, Y. Kobayashi, K. Torizuka, T. Homma, and H. Takahashi, Appl. Phys. B, Lasers Opt. **74**, S43 (2002).
[47] M. Kakehata, H. Takada, Y. Kobayashi, K. Torizuka, Y. Fujihira, T. Homma, and H. Takahashi, Opt. Lett. **26**, 1436 (2001).
[48] A. Baltuška, M. Uiberacker, E. Goulielmakis, R. Kienberger, V. S. Yakovlev, T. Udem, T. W. Hänsch, and F. Krausz, IEEE J. Quantum Electron. **9**, 972 (2003).
[49] C. Corsi and M. Bellini, Appl. Phys. B, Lasers Opt. **78**, 31 (2004).
[50] M. G. Schätzel, F. Lindner, G. G. Paulus, H. Walther, E. Goulielmakis, A. Baltuška, M. Lezius, and F. Krausz, Appl. Phys. B, Lasers Opt. **79**, 1021 (2004).
[51] I. Thomann, E. Gagnon, R. J. Jones, A. S. Sandhu, A. Lytle, R. Anderson, J. Ye, M. M. Murnane, and H. C. Kapetyn, Opt. Express **12**, 3493 (2004).
[52] M. Kakehata, H. Takada, Y. Kobayashi, K. Torizuka, H. Takamiya, K. Nishijima, T. Homma, H. Takahashi, K. Okubo, S. Nakamura, and Y. Koyamada, Opt. Express **12**, 2070 (2004).
[53] Z. Chang, Appl. Opt. **45**, 8350 (2006).
[54] C. Li, E. Moon, and Z. Chang, Opt. Lett. **31**, 3113 (2006).
[55] C. Li, E. Moon, H. Mashiko, C. M. Nakamura, P. Ranitovic, C. M. Maharjan, C. L. Cocke, Z. Chang, and G. G. Paulus, Opt. Express **14**, 11468 (2006).
[56] B. Shan, C. Wang, and Z. Chang, U. S. Patent No. 7,050,474 (23 May 2006).
[57] C. Li, H. Mashiko, H. Wang, E. Moon, S. Gilbertson, and Z. Chang, Appl. Phys. Lett. **92**, 191114 (2008).
[58] H. Wang, C. Li, J. Tackett, H. Mashiko, C. M. Nakamura, E. Moon, and Z. Chang, Appl. Phys. B, Lasers Opt. **89**, 275 (2007).
[59] C. Li, E. Moon, H. Wang, H. Mashiko, C. M. Nakamura, J. Tackett, and Z. Chang, Opt. Lett. **32**, 796 (2007).
[60] C. Li, E. Moon, H. Mashiko, H. Wang, C. M. Nakamura, J. Tackett, and Z. Chang, Appl. Opt. **48**, 1303 (2009).
[61] P. Corkum and F. Krausz, Attosecond science, Nature Phys. **3**, 381(2007).
[62] M. F. Kling and M. J. J. Vrakkking, Attosecond electron dynamics, Annu. Rev. Phys. Chem. **59**, 463 (2008).
[63] P. Salières, A. L'Huillier, P. Antoine, and M. Lewenstein, Adv. Atom. Mol. Opt. Phys. **41**, 83 (1999).
[64] P. B. Corkum, Phys. Rev. Lett. **71**, 1994 (1993).
[65] K. C. Kulander, K. J. Schafer, and J. L. Krause, Super-Intense Laser-Atom Physics, NATO ASI, Ser. B, Vol. 316 (Plenum, New York, 1993), p. 95.
[66] P. M. Paul, E. S. Toma, P. Breger, G. Mullot, F. Auge, Ph. Balcou, H. G. Muller, and P. Agostini, Science **292**, 1689 (2001).
[67] E. Goulielmakis, M. Schultze, M. Hofstetter, V. S. Yakovlev, J. Gagnon, M. Uiberacker, A. L. Aquila, E. M. Gullikson, D. T. Attwood, R. Kienberger, F. Krausz, and U. Kleinberg, Science **320**, 1614 (2008).
[68] P. B. Corkum, N. H. Burnett, and M. Y. Ivanov, Opt. Lett. **19**, 1870 (1994).
[69] Z. Chang, Phys. Rev. A **70**, 043802 (2004).
[70] G. Sanssone, E. Benedetti, F. Calegari, C. Vozzi, L. Avaldi, R. Flammini, L. Poletto, P. Villoresi, C. Altucci, R. Velotta, S. Stagira, S. De Silvestri, and M. Nisoli, Science **314**, 443 (2006).
[71] S. Gilbertson, H. Mashiko, C. Li, E. Moon, and Z. Chang, Appl. Phys. Lett. **93**, 111105 (2008).
[72] H. M. Crespo, J. R. Birge, E. L. Falcão-Filho, M. Y. Sander, A. Benedick, and F. X. Kärtner, Opt. Lett. **33**, 833 (2008).